

Wavepacket control and simulation protocol for entangled two-photon-absorption of molecules

Bing Gu,^{*} Daniel Keefer, and Shaul Mukamel[†]

*Department of Chemistry & Department of Physics and Astronomy,
University of California, Irvine, California, 92697, USA*

Quantum light spectroscopy, providing novel molecular information non-accessible by classical light, necessitates new computational tools when applied for complex molecular systems. We introduce two computational protocols for the molecular nuclear wave packet dynamics interacting with an entangled photon pair to produce the entangled two-photon absorption signal. The first involves summing over transition pathways in a temporal grid defined by two light-matter interaction times accompanied by the field correlation functions of quantum light. The signal is obtained by averaging over the two-time distribution characteristic of the entangled photon state. The other protocol involves a Schmidt decomposition of the entangled light and requires summing over the Schmidt modes. We demonstrate how photon entanglement can be used to control and manipulate the two-photon excited nuclear wave packets in a displaced harmonic oscillator model.

I. INTRODUCTION

Numerous novel spectroscopic techniques which exploit the variation of photon statistics upon interaction with matter are made possible by quantum light [1, 2]. Such quantum spectroscopy has been demonstrated, both theoretically and experimentally, to be a powerful technique that can reveal molecular information not accessible by classical light [2] and can further enhance the signal-to-noise ratio and resolution beyond the classical limit [3]. The incoming photon statistics can be employed as a novel control knob for the optical response functions of matter [4, 5]. Quantum optical effects such as the Hong-Ou-Mandel two-photon interference [6] can be used to generate signals which have no classical analogs [7–9].

^{*} bingg@uci.edu

[†] smukamel@uci.edu

Entangled two-photon absorption (ETPA) has recently attracted considerable attention [10–26]. The extent to which two-photon absorption rate can be enhanced by entangled light is under debate. While several ETPA experiments have been reported [27, 28], a recent theoretical analysis shows that ETPA events is below the detection level for typical molecular systems in realistic experimental setup [10]. In ETPA, a molecule is promoted from the ground state to an excited state by simultaneously absorbing two, degenerate or nondegenerate, photons. This technique drastically differs from classical two-photon absorption. At low photon fluxes, it scales linearly, rather than quadratically with the pump photon intensity [24, 29]. This is because the entangled photon pair generated by e.g. spontaneous parametric downconversion [30–33] is created simultaneously and thus interacts with molecules at the same time. Furthermore, when a narrowband pump is utilized in the twin-photon generation, they exhibit a strong frequency-anticorrelation, i.e., detection of one photon reveals the frequency of its twin within a small uncertainty determined by the pump bandwidth. This energy-time entanglement can be used in spectroscopy to manipulate the quantum interference among transition pathways, which have been shown to induce classically disallowed collective excitations [34], and to probe classically-dark bipolariton states [20]. Since the ETPA signal depends on the entangled photon pair statistics, the biphoton joint spectral amplitude can be used to optimize the two-photon excitation process, leading to quantum control by entangled light [35]. Early applications have focused on controlling the electronically excited-state populations in model systems with frozen nuclear motion [35]. However, nuclear motions are responsible for reactive dynamics initiated by two-photon absorption, especially for molecules passing through conical intersections with strong vibrational-electronic (vibronic) coupling.

To fully describe the coupled electron-vibration-photonic dynamics, we develop a computational framework involving molecular nuclear wave packet quantum dynamics interacting with quantum light. While the response to classical laser pulses can be obtained by solving the time-dependent Schrödinger equation, this is not the case for quantum light.

Our simulation protocol, based on time-dependent perturbation theory for the light-matter interaction, involves summing over all two-photon transition pathways in a two-dimensional temporal grid defined by the two interaction times with the entangled photon pair. Using a displaced harmonic oscillator model widely used to describe vibronic transitions [36], we demonstrate how photon entanglement, a novel control knob not available for classical light, can be utilized to control the nuclear

wave packet in electronically excited states. Three scenarios are examined whereby the intermediate electronic state is resonant, off-resonant, and, far off-resonant with the incoming photons. We find that the two-photon-excited population is largest for the resonant case. A linear dependence of the final-state population on the entanglement time is found for short entanglement times. This observation is rationalized by an analytical analysis based on sum-over-states expression. We further demonstrate that entanglement provides a useful control knob for the two-photon excited wave packets. Modulating the entanglement time has the strongest effect on the shape of created nuclear wave packet in the off-resonant case.

II. THEORY AND COMPUTATION

A. The entangled two-photon absorption signal

We consider a molecule-photon system described by the Hamiltonian ($\hbar = e = 4\pi\epsilon_0 = 1$)

$$H = H_M + H_R + H_{RM}. \quad (1)$$

The molecular Hamiltonian $H_M = T_n + H_{BO}(\mathbf{R})$ represents the vibronic dynamics where T_n is the nuclear kinetic energy operator, $H_{BO}(\mathbf{R}) = \sum_\alpha V_\alpha(\mathbf{R}) |\psi_\alpha(\mathbf{R})\rangle \langle \psi_\alpha(\mathbf{R})|$ the adiabatic (Born-Oppenheimer) electronic Hamiltonian with $V_\alpha(\mathbf{R})$ being the α th potential energy surface (PES). The radiation Hamiltonian

$$H_R = \sum_{j=s, i} \int_0^\infty d\omega \hbar\omega \left(a_j^\dagger(\omega_j) a_j(\omega_j) + \frac{1}{2} \right) \quad (2)$$

represents two continua of photon modes, signal and idler, generated by a SPDC process, $H_{RM} = \sum_j -\boldsymbol{\mu} \cdot \mathbf{E}_j(\mathbf{r})$ is the light-matter interaction in the electric dipole approximation, where $\mathbf{E}_j(\mathbf{r}) = \mathbf{E}_j^{(+)}(\mathbf{r}) + \mathbf{E}_j^{(-)}(\mathbf{r})$ and

$$\mathbf{E}_j^{(+)}(\mathbf{r}) = i \int_0^\infty d\omega \mathcal{E}(\omega) \mathbf{e}_j a_j(\omega) e^{-i\mathbf{k} \cdot \mathbf{r}} \quad (3)$$

the electric field operator of the j th photon beam with polarization \mathbf{e}_j at molecular location \mathbf{r} , and $\mathcal{E}(\omega) \equiv \sqrt{\frac{2\pi\omega}{cnA}}$ with the beam transversal area A , the refractive index n , and the speed of light

c. The joint electron-nuclei-photonic space is given by the tensor product of the electron-nuclear Hilbert space and the photon modes Fock space. The joint light-matter state is

$$|\Psi(t)\rangle = \sum_{\alpha, \mathbf{n}} |\psi_{\alpha}(\mathbf{R})\rangle |\chi_{\alpha, \mathbf{n}}(t)\rangle |n(\omega) \dots\rangle \quad (4)$$

where $|\psi_{\alpha}(\mathbf{R})\rangle$ is the adiabatic electronic state, $\chi_{\alpha, \mathbf{n}}(\mathbf{R}, t)$ the nuclear wavefunction at the α th electronic state and the photon state is described in the occupation number representation $|\mathbf{n}\rangle \equiv |n(\omega)n(\omega') \dots\rangle$. The initial state of the joint light-matter system is $|\psi_0(\mathbf{R})\rangle |\chi_0\rangle |\Phi_0\rangle$ where $|\Phi_0\rangle$ describes the quantum light. The probability to arrive at the final electronic state $|\psi_f\rangle$ at time t is given by

$$P(t) = \int d\mathbf{R} \langle \Psi(t) | |\psi_f(\mathbf{R}), \mathbf{R}\rangle \langle \psi_f(\mathbf{R}), \mathbf{R} | \otimes |0\rangle \langle 0 | | \Psi(t)\rangle = \int d\mathbf{R} |\chi_f(\mathbf{R}, t)|^2 \quad (5)$$

where

$$\chi_f(\mathbf{R}, t) = \langle \psi_f(\mathbf{R}), \mathbf{R} | \otimes \langle 0 | | \Psi(t)\rangle \quad (6)$$

is the nuclear wavefunction for the final electronic state created by the two-photon excitation process where the photon modes are in the vacuum state $|0\rangle$. This is obtained by projecting the total state onto the final electronic state and the photon vacuum after the pump pulse $t > t_p$. The joint light-matter state at time t is obtained using time-dependent perturbation theory in the light-matter interaction in the interaction picture of $H_0 = H_M + H_R$. To second-order, we have

$$|\tilde{\Psi}(t)\rangle = - \sum_{i,j} \int_{t_0}^t dt_2 \int_{t_0}^{t_2} dt_1 (\boldsymbol{\mu}(t_2) \cdot \mathbf{e}_j) (\boldsymbol{\mu}(t_1) \cdot \mathbf{e}_i) |\psi_0\rangle |\chi_0\rangle E_j^{(+)}(t_2) E_i^{(+)}(t_1) |\Phi_0\rangle \quad (7)$$

where $A(t) = U_0^\dagger(t) A U_0(t)$ is the operator A in the interaction picture, i, j are the beam indices, and $|\tilde{\Psi}(t)\rangle = U_0^\dagger(t) |\Psi(t)\rangle$. We consider two incoming beams and neglect the zero- (no interaction) and first-order (one-photon) processes in Eq. (7) as they do not contribute to the two-photon absorption. The dipole operator acts in the joint electron-nuclear space

$$\boldsymbol{\mu} = \sum_{\alpha \neq \beta} \int d\mathbf{R} \langle \psi_{\beta}(\mathbf{R}) | \boldsymbol{\mu} | \psi_{\alpha}(\mathbf{R}) \rangle_{\mathbf{r}} |\psi_{\beta}(\mathbf{R}), \mathbf{R}\rangle \langle \psi_{\alpha}(\mathbf{R}), \mathbf{R} | \quad (8)$$

where α, β labels the electronic states and $\langle \dots \rangle_{\mathbf{r}}$ refers to integrating over electronic degrees of freedom. We further assume that the molecule has no permanent dipole moments so that $\alpha \neq \beta$.

Inserting Eq. (7) into Eq. (6) yields

$$\tilde{\chi}_f(\mathbf{R}, t) = - \sum_{i,j} \sum_e \int_{t_0}^t dt_2 \int_{t_0}^{t_2} dt_1 V_{fe}^{(j)}(\mathbf{R}, t_2) V_{eg}^{(i)}(\mathbf{R}, t_1) \chi_0(\mathbf{R}) \Phi_{ji}(t_2, t_1) \quad (9)$$

where $V_{\beta\alpha}^{(j)}(\mathbf{R}) = \langle \psi_\beta(\mathbf{R}) | \boldsymbol{\mu} \cdot \mathbf{e}_j | \psi_\alpha(\mathbf{R}) \rangle_{\mathbf{r}}$ is the transition dipole moment projected on the polarization of j th photon beam, e runs over all intermediate electronic surfaces, and

$$\Phi_{ji}(t_2, t_1) = \langle 0 | E_j^{(+)}(t_2) E_i^{(+)}(t_1) | \Phi_0 \rangle \quad (10)$$

is the entangled two-photon transition amplitude. Transforming back to the Schrodinger picture we obtain

$$\begin{aligned} \chi_f(\mathbf{R}, t) &= - \sum_{i,j} \sum_e \int_{t_0}^t dt_2 \int_{t_0}^{t_2} dt_1 \xi(t_2, t_1) \\ \xi(t_2, t_1) &\equiv U_f(t, t_2) V_{fe}^{(j)}(\mathbf{R}) U_e(t_2, t_1) V_{eg}^{(i)}(\mathbf{R}) U_g(t_1, t_0) \chi_0(\mathbf{R}) \Phi_{ji}(t_2, t_1) \end{aligned} \quad (11)$$

where $U_M(t, t') = e^{-iH_M(t-t')}$ is the molecular free propagator. The wave packet $\xi(t_2, t_1)$ represents a single two-photon-absorption event with two light-matter interactions occurring at t_1 and t_2 . This reduces to the $|g\rangle \rightarrow |f\rangle$ transition amplitude if the nuclear motion is frozen.

Using the Feynman diagram Fig. 1, Eq. (11) can be interpreted as follows: The final nuclear wave packet at time t on the f th PES is given by a sum over of all possible transition pathways. Each pathway contains two dipole interaction times t_1 and t_2 , where the molecule undergoes a transition between electronic states. Between t_0 and t_1 , the molecule remains at the ground state. At t_1 , the molecule makes a transition to the e th electronic state, launching a nuclear wave packet dynamics until it interacts with the second photon at t_2 , which brings it to the final f -PES. Nuclear dynamics then takes place between t_2 and the final time t on this PES. Each two-photon transition pathway depends on the two-photon transition amplitude $\Phi_{ji}(t_2, t_1)$, whose modulus squared gives the probability of detecting the i -photon at time t_1 and j -photon at t_2 . The molecule thus serves as a photodetector [37]. The dependence of the ETPA signal on the photon statistics allows to control the two-photon excited nuclear wave packet on the excited-state PES by shaping the two-photon wave function.

B. Energy-Time entangled light

The two-photon wavefunction is described by the joint spectral amplitude (JSA) of the entangled photon pair. Here we employ the twin-photon, signal and idler, state, generated by a type-II SPDC

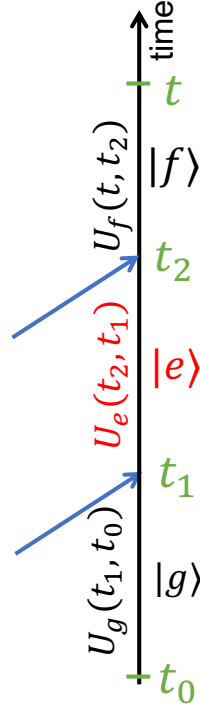


FIG. 1. Feynman diagram representing Eq. (11). $|g\rangle$, $|e\rangle$, $|f\rangle$ represent the ground, intermediate, and final electronic states. The $U_\alpha(t, t') = e^{i(T_n + V_\alpha(\mathbf{R}))(t-t')}$ is the free-molecule propagator on the α th PES. Between t_0 and t_1 , the molecule remains in the ground state. The first photon, either signal and idler, brings the molecule to the intermediate state, launching nuclear dynamics on the associated PES.

process [26, 31, 32],

$$|\Phi\rangle = \iint_0^\infty d\omega_s d\omega_i J(\omega_s, \omega_i) a_s^\dagger(\omega_s) a_i^\dagger(\omega_i) |0\rangle \quad (12)$$

where the JSA $J(\omega_s, \omega_i)$ is the amplitude of detecting the signal photon with frequency ω_s and idler photon with frequency ω_i , and $a_j(\omega)$ ($a_j^\dagger(\omega)$) annihilates (creates) a j -photon with frequency ω satisfying the boson commutation relation $[a_j(\omega), a_{j'}^\dagger(\omega')] = \delta_{jj'} \delta(\omega - \omega')$. We focus on the frequency anti-correlation of the entangled photons, and suppress the spatial degrees of freedom [32, 38]. For a Gaussian pump with central frequency $\bar{\omega}_p$ and bandwidth σ_p , the JSA reads

$$J(\omega_1, \omega_2) = \mathcal{N} \exp\left(-\frac{(\omega_1 + \omega_2 - \bar{\omega}_p)^2}{4\sigma_p^2}\right) \text{sinc}\left(\frac{\Delta k L}{2}\right) \quad (13)$$

where L is the crystal length, $\Delta k = k_s(\omega_s) + k_i(\omega_i) - k_p(\omega_s + \omega_i)$ is the wavenumber mismatch and $k_j = n_j(\omega_j)\omega_j/c$, \mathcal{N} is the normalization factor ensuring $\iint d\omega_s d\omega_i |J(\omega_s, \omega_i)|^2 = 1$, and $\text{sinc}(x) = \frac{\sin(x)}{x}$. We focus on the degenerate state where the central frequencies for the signal and idler photons

are identical $\bar{\omega}_s = \bar{\omega}_i = \frac{1}{2}\bar{\omega}_p$. Taylor expansion of the wave number gives $k_j(\omega_j) \approx k_j(\bar{\omega}_j) + \Delta_j/v_j$ where $\Delta_j = \omega_j - \bar{\omega}_j$ and $v_j \equiv \frac{d\omega_j}{dk_j}$ is the group velocity of j th beam. Under the phase matching condition $k_s(\bar{\omega}_s) + k_i(\bar{\omega}_i) - k_p(\bar{\omega}_p) = 0$, the JSA becomes

$$J(\Delta_s, \Delta_i) = \mathcal{N} \exp\left(-\frac{(\Delta_s + \Delta_i)^2}{4\sigma_p^2}\right) \text{sinc}\left(\frac{1}{2}\bar{T}(\Delta_s + \Delta_i) + \frac{1}{2}(\Delta_s - \Delta_i)T_e\right) \quad (14)$$

where $T_e = \frac{1}{2}\left(\frac{L}{v_s} - \frac{L}{v_i}\right)$ is the entanglement time characterizing the difference between the arrival times of the photon pair and $\bar{T} = \frac{1}{2}\left(\frac{L}{v_s} + \frac{L}{v_i}\right) - \frac{L}{v_p}$ is the travel time difference between the biphoton and the pump inside the nonlinear crystal. The twin-photon JSA for different entanglement times are shown in Fig. 2. Each photon bandwidth is controlled by the entanglement time with shorter T_e leading to broader bandwidth, whereas the sum frequency of the signal and idler beams are narrowly distributed independent of the bandwidth of individual photon.

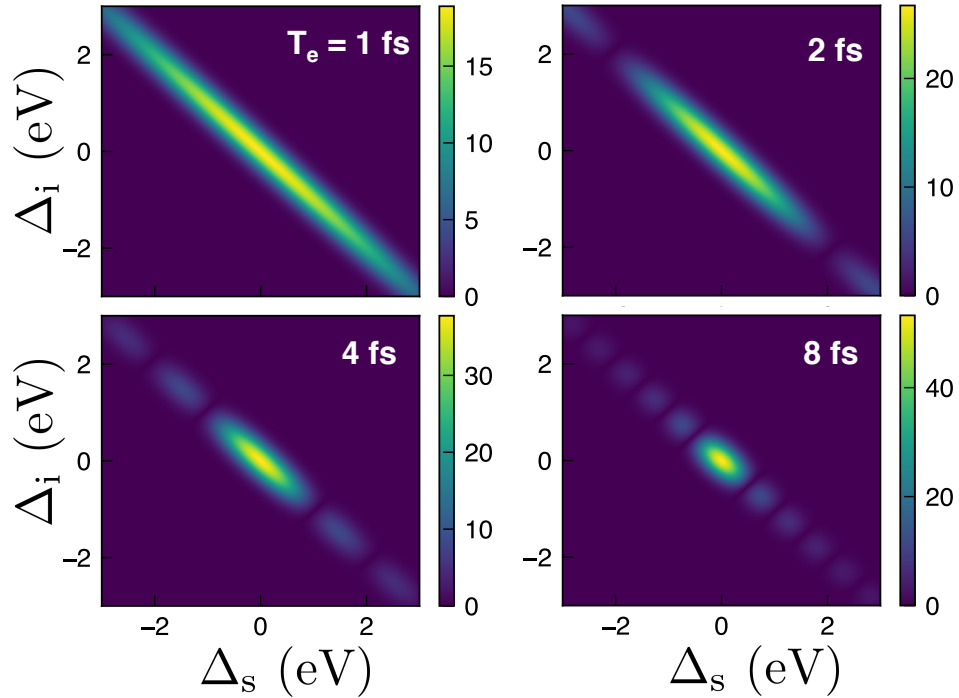


FIG. 2. The joint spectral amplitude $|J(\Delta_s, \Delta_i)|$ of the quantum light [Eq. (14)] for different entanglement times T_e . Here $\sigma_p = 0.2$ eV, $\bar{T} = 0$.

The two-photon detection amplitude is given by

$$\Phi_{\text{is}}(t_2, t_1) = \iint_0^\infty d\omega_s d\omega_i \mathcal{E}(\omega_i) \mathcal{E}(\omega_s) e^{-i\omega_i t_2 - i\omega_s t_1} f(\omega_s, \omega_i) \quad (15)$$

Invoking the narrowband limit $\mathcal{E}(\omega_j) \approx \mathcal{E}(\bar{\omega}_j)$, changing the variables to Δ_j and extending the integration range to $(-\infty, \infty)$, yields

$$\Phi_{\text{is}}(t_2, t_1) = (2\pi)^2 \mathcal{E}(\bar{\omega}_i) \mathcal{E}(\bar{\omega}_s) \exp(-i\bar{\omega}_i t_2 - i\bar{\omega}_s t_1) J(t_1, t_2) \quad (16)$$

where $J(t_1, t_2) = \iint_{-\infty}^{\infty} \frac{d\Delta_s d\Delta_i}{(2\pi)^2} J(\Delta_s, \Delta_i) e^{-i\Delta_i t_2 - i\Delta_s t_1}$ is the joint temporal amplitude of the twin-photons. For $\bar{T} = 0$,

$$J(t_1, t_2) = \sqrt{\sigma_p/T_e} (2\pi)^{-5/4} e^{-\sigma_p^2(t_1+t_2)^2/4} \Pi\left(\frac{t_1 - t_2}{2T_e}\right) \quad (17)$$

where $\Pi(x) = 1$ for $|x| < \frac{1}{2}$ and 0 otherwise.

C. Simulation Protocol Based on a Time Grid

Equation (11) suggests the following simulation protocol: we first sample (t_2, t_1) on a two-dimensional triangular grid with t_2 ranging from t_0 to the final time t , and t_1 samples t_0 to t_2 ; for each (t_1, t_2) , we compute the nuclear wave packet $\xi(t_2, t_1)$ by a wave packet dynamics solver. The final wave packet can then be obtained by a sum over all $\xi(t_2, t_1)$.

The final nuclear wave packet Eq. (11) is simulated as follows (for brevity, we assume a single intermediate electronic state e):

1. Set the initial wave packet to $\chi_e(\mathbf{R}) = \mu_{eg}(\mathbf{R})\chi_0(\mathbf{R})$
2. Propagate the wave packet on the e th PES for time interval τ leading to $\chi_e(\mathbf{R}, \tau) = U_M(\tau)\mu_{eg}(\mathbf{R})\chi_0(\mathbf{R})$.
3. Using Eq. (15), perform the following integration to obtain an auxiliary wavepacket $\zeta(\mathbf{R}, t)$,

$$\zeta(\mathbf{R}, \tau_2) = \int_0^{\tau_2} d\tau \Phi(\tau_2 + t_0, \tau_2 - \tau + t_0) \chi_e(\mathbf{R}, \tau) \quad (18)$$

4. For each $\tau_2 = t - t_0 - t_2$, apply the dipole operator to $\zeta(\mathbf{R}, \tau_2)$ that brings the molecule to the final electronic state, $\mu_{fe}(\mathbf{R})\zeta(\mathbf{R}, \tau_2)$, and propagate the wave packet for $t - t_0 - \tau_2$ on the final PES. Summing up all possible τ_2 leads to

$$\chi_f(\mathbf{R}, T = t - t_0) = \int_0^T d\tau_2 U_M(t - t_0 - \tau_2) \mu_{fe}(\mathbf{R}) \zeta(\mathbf{R}, \tau_2) \quad (19)$$

The molecular propagator is computed using a wave packet dynamics on a single PES [39]. The second-order split-operator method is employed for adiabatic wave packet dynamics on a single PES $V_\alpha(\mathbf{R})$. A Trotter decomposition of the propagator is employed

$$U_\alpha(\delta t) = e^{-iV_\alpha\delta t/2} e^{-iT_n\delta t} e^{-iV_\alpha\delta t/2} + \mathcal{O}((\delta t)^3) \quad (20)$$

for a short time interval δt and fast Fourier transform switching the wavefunction between the coordinate and momentum space.

III. RESULTS AND DISCUSSION

Simulations were carried out for a three-state displaced harmonic oscillator model with a single nuclear coordinate x and corresponding momentum p . The PESs depicted in Fig. 3 are given by

$$V_\alpha(x) = \frac{p^2}{2} + \frac{\omega_\alpha^2}{2} (x - d_\alpha)^2 + E_\alpha \quad (21)$$

where $\alpha = \{g, e, f\}$ referring to the ground, intermediate, and final electronic states, respectively, and d_α is the displacement, and E_α is the zero-phonon line. By tuning the energy E_e , we cover three scenarios whereby the intermediate PES is resonant, off-resonant and far off-resonant with respect to the incoming photons. Other parameters are $E_g = 0$, $E_f = 2$ eV, $d_g = 0$, $d_e = -d_f = -10a_0$.

A. Sum-over-states expansion of the molecular response

We explore the variation of the electronic populations and wave packets with the entanglement time by employing the sum-over-states expression for the molecular response in the vibronic eigenstates of the molecular Hamiltonian H_M . Let $|\alpha\nu\rangle$ denote the vibronic states associated with α th electronic state with eigenenergies $\omega_{\alpha\nu}$, the molecular propagator and the interaction picture dipole operator is $U_M(t) = \sum_\alpha \sum_\nu e^{-i\omega_{\alpha\nu}t} |\alpha\nu\rangle \langle\alpha\nu|$ and $V^{(j)}(t) = \sum_{\beta\nu',\alpha\nu} V_{\beta\nu',\alpha\nu}^{(j)} e^{i\omega_{\beta\nu',\alpha\nu}t} |\beta\nu'\rangle \langle\alpha\nu|$ with $\omega_{\beta\nu',\alpha\nu} = \omega_{\beta\nu'} - \omega_{\alpha\nu}$. Inserting these into Eq. (11) yields $|\chi_f(t)\rangle = \sum_\nu A_{f\nu,g0}(t) |f\nu\rangle$ where

$$T_{f\nu,g0}(t) = (2\pi)^2 \mathcal{E}(\bar{\omega}_i) \mathcal{E}(\bar{\omega}_s) \sum_{e,\nu'} \mu_{f\nu,e\nu'}^{(i)} \mu_{e\nu',g0}^{(s)} \int_{t_0}^t dt_2 e^{i(\omega_{f\nu,e\nu'} - \bar{\omega}_i)t_2} \int_{t_0}^{t_2} dt_1 e^{i(\omega_{e\nu',g0} - \bar{\omega}_s)t_1} J(t_1, t_2) \quad (22)$$

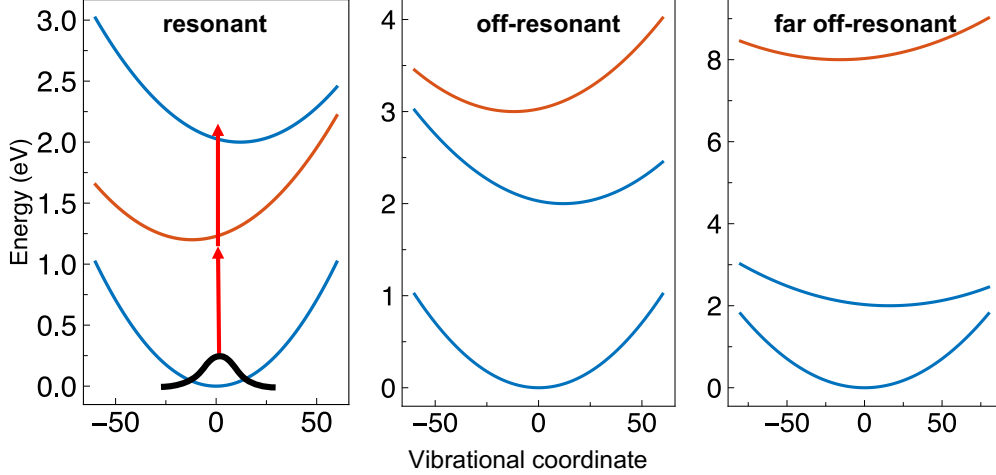


FIG. 3. Potential energy surfaces of the displaced harmonic oscillator model corresponding to three different cases where the intermediate electronic state is resonant, off-resonant, and far off-resonant with the incoming photons. Correspondingly, $E_e = 1.2, 3, 8$ eV.

is the transition amplitude from the ground vibrational state in the ground electronic state PES $|g0\rangle$ to the vibronic state $|f\nu\rangle$. Using Eq. (17) and taking $t \rightarrow \infty, t_0 \rightarrow -\infty$ yields

$$A_{f\nu,g0} = (2\pi)^{3/4} \sqrt{\frac{\pi}{\sigma_p T_e}} \mathcal{E}(\bar{\omega}_i) \mathcal{E}(\bar{\omega}_s) \exp\left(-\frac{(\omega_{f\nu,g0} - \bar{\omega}_p)^2}{4\sigma_p^2}\right) \sum_{\nu'} \mu_{f\nu,e\nu'}^{(i)} \mu_{e\nu',g0}^{(s)} \frac{e^{i\Delta_{\nu'} T_e} - 1}{i\Delta_{\nu'}} + (s \leftrightarrow i) \quad (23)$$

where ν' runs over the vibrational eigenstates in e th PES, $\Delta_{\nu'} = \frac{1}{2}\omega_{f\nu,g0} - \omega_{e\nu',g0}$ and $\mu_{\beta\nu',\alpha\nu} = \langle \beta\nu' | \mu | \alpha\nu \rangle$ is the transition dipole moment between vibronic states.

Fig. 4 depicts the two-photon-excited population as a function of the entanglement time. The largest excited population occurs for the resonant case (upper panel), as reflected in the detuning factor $1/\Delta_{\nu'}$ in Eq. (23). Interestingly, the population grows, roughly linearly, with T_e at short entanglement times. To rationalize this observation, we isolate the T_e -dependent factor in Eq. (23) $g(T_e) = \frac{1}{\sqrt{T_e}} \frac{e^{i\Delta_{\nu'} T_e} - 1}{i\Delta_{\nu'}}$ and we use $e^x \approx 1 + x$

$$P \propto |g(T_e)|^2 \approx T_e. \quad (24)$$

Thus, for resonant intermediate states and short entanglement times, the two-photon-excited population grows linearly with T_e . After the first photon interacts with the molecules, transient population is built in the intermediate state. This population grows for a short period of time until

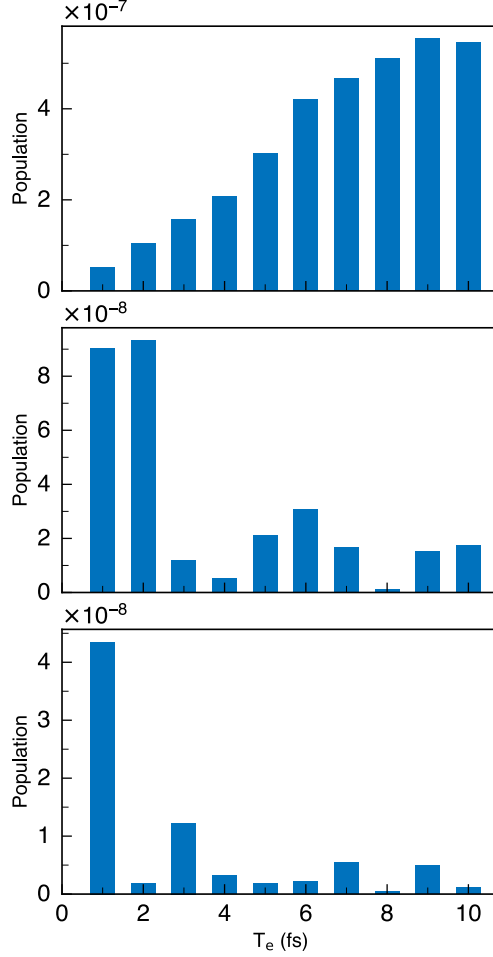


FIG. 4. Dependence of the entangled two-photon-excited population on the entanglement time. The parameters read $A = 1\mu\text{m}^2$, $n = 1$, $\bar{\omega}_p = 2.4\text{ eV}$, $\sigma_p = 0.2\text{ eV}$.

the second photon arrives. The time window is bounded by the entanglement time of the quantum light, whereas for classical light there is no such restriction. This linear increase only exists at very short entanglement times below $T_e = 10\text{ fs}$.

For off-resonant and far off-resonant intermediate states (middle and lower panels of Fig. 4), the two-photon-excited population shows a nonlinear dependence on the entanglement time. In both cases the largest population occurs at short entanglement times with the population for the off-resonant case larger than the far off-resonant case, as expected.

Apart from controlling the electronic populations, the JSA may also be used to manipulate the nuclear wave packet. Figs. 5, 6, and 7 show the phase-space Wigner representation of the nuclear

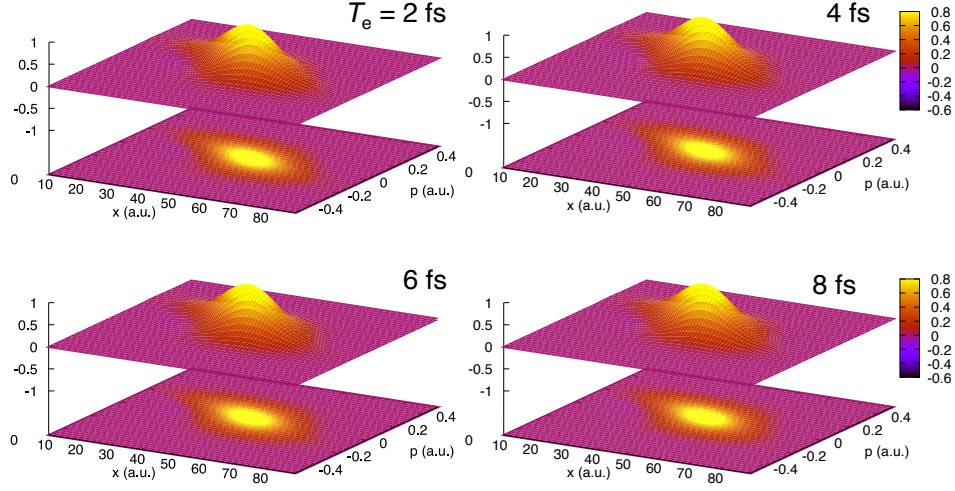


FIG. 5. Phase space representation of entangled two-photon-excited wavepackets for the displaced harmonic oscillator model with a resonant intermediate electronic state for various entanglement times as indicated.

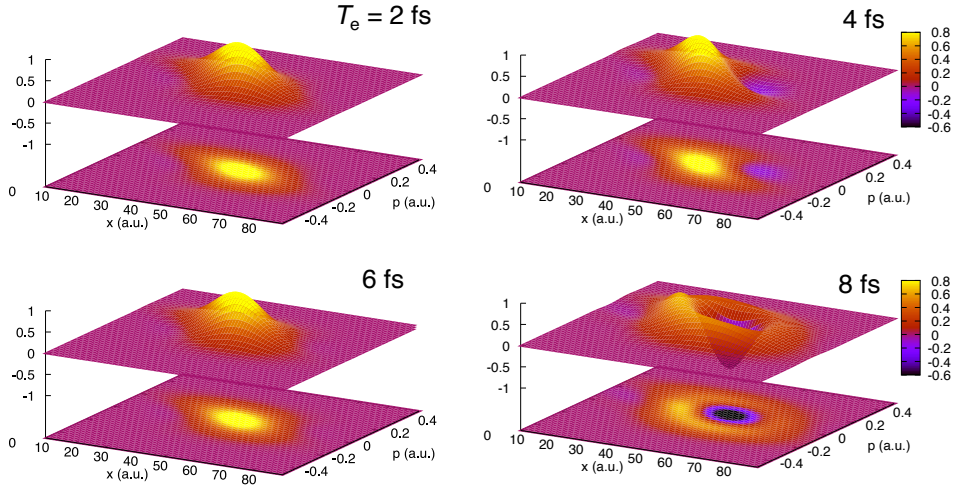


FIG. 6. Same as Fig. 5 but for off-resonant intermediate electronic state.

wave packets prepared by entangled light with various entanglement times at $t = 20$ fs for the resonant, off-resonant, and far off-resonant cases, respectively. The Wigner spectrogram transforms the wavepacket in coordinate space as $\chi_w(x, p, t) = \int_{-\infty}^{\infty} dy \chi_f(x + \frac{y}{2}) \chi_f^*(x - \frac{y}{2}) e^{ipy}$. We see that the nuclear wavepacket is most sensitive to the entanglement time in the off-resonant case with minor variations otherwise. The nuclear wave packet depends on both the amplitude and phase of

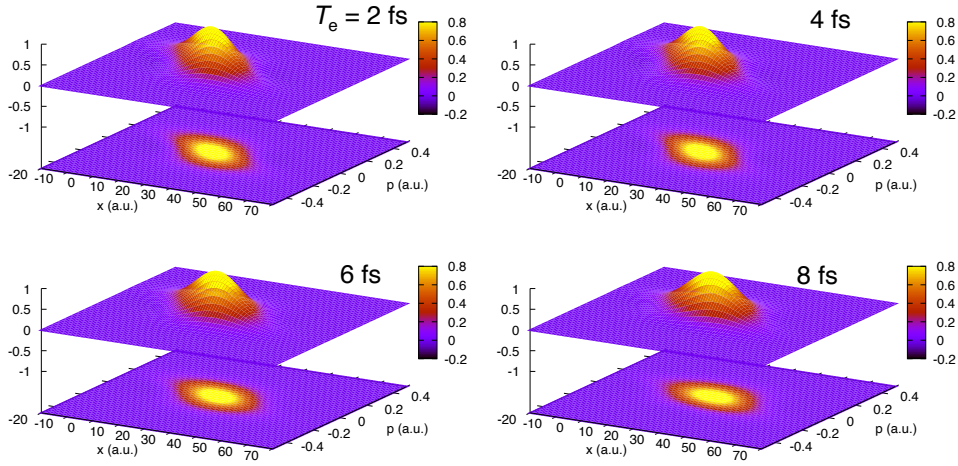


FIG. 7. Same as Fig. 5 but for far off-resonant intermediate electronic state.

the transition amplitude to a vibronic state in the f th electronic state $A_{f\nu}$. For the resonant case, Eq. (24) implies that for short entanglement times, the relative phase between vibrational states in the f -PES does not depend on T_e . For the off-resonant case, the $g(T_e)$ will show an oscillatory behavior with T_e and the relation between $A_{f\nu}$ and the vibrational state ν will strongly depend on T_e thus leading to a considerable change in the wavepacket.

B. Simulation Protocol Based on the Schmidt decomposition

Sampling the wavepackets on the two-dimensional time grid is numerically expensive. We now present an alternative simulation protocol for the ETPA, which employs the Schmidt decomposition of the entangled light [40] and replaces the time grid sampling by a summation over Schmidt modes. The entangled light can be expanded in Schmidt modes. Each pair of modes leads to a transition amplitude, and summing over all contributing Schmidt modes leads to the final signal. The photon-pair entanglement is then reflected in the quantum interference among Schmidt modes.

1. *Schmidt decomposition of quantum light*

With the Schmidt decomposition for the JSA [40, 41], $J(\omega_s, \omega_i) = \sum_n \sqrt{\lambda_n} \phi_n(\omega_s) \varphi_n(\omega_i)$, the two-photon wavefunction can then be expressed by

$$\Phi_{\text{is}}(t_2, t_1) = (2\pi)^2 \mathcal{E}(\bar{\omega}_i) \mathcal{E}(\bar{\omega}_s) \sum_n \sqrt{\lambda_n} \phi_n(t_1) \varphi_n(t_2) \quad (25)$$

where $\phi_n(t) = \int_{-\infty}^{\infty} \frac{d\omega}{2\pi} \phi_n(\omega) e^{i\omega t}$ and $\varphi_n(t)$ are the temporal modes, i.e., Schmidt modes Fourier transformed to the time domain, $\phi_n(\omega_s)$ and $\varphi_n(\omega_i)$ are Schmidt modes, that are, respectively, the eigenstates of the reduced density matrices of the signal and idler photons with λ_n the corresponding eigenvalues.

Inserting Eq. (25) into Eq. (11) leads to

$$\begin{aligned} \chi_f(\mathbf{R}, t) &= (2\pi)^2 \mathcal{E}(\bar{\omega}_i) \mathcal{E}(\bar{\omega}_s) \sum_n \sqrt{\lambda_n} \kappa_n(\mathbf{R}, t) \\ \kappa_n(\mathbf{R}, t) &\equiv \sum_e \int_{t_0}^t dt_2 \int_{t_0}^{t_2} dt_1 U_f(t, t_2) V_{fe}^\dagger(\mathbf{R}) U_e(t_2, t_1) V_{eg}^\dagger(\mathbf{R}) \chi_0(\mathbf{R}) \phi_n(t_1) \varphi_n(t_2) \end{aligned} \quad (26)$$

$\kappa_n(\mathbf{R}, t)$ is the two-photon-excited nuclear wavepacket with the n th pair of Schmidt modes. An important observation is that the κ_n can be simply simulated by solving time-dependent Schrödinger equation in the presence of two classical pulses with electric field $\mathcal{E}_s(t) = \phi_n(t)$, $\mathcal{E}_i(t) = \varphi_n(t)$. Therefore, instead of using a temporal grid one can simply solve the time-dependent Schrödinger equation to compute the ETPA signal.

However, in classical two-photon absorption, there are additional second-order transition pathways corresponding to absorbing two photons from a single beam, which does not exist in quantum light. This becomes clear in the classical TPA expression

$$\chi_f(\mathbf{R}, t) \propto \int_{t_0}^t dt_2 \int_{t_0}^{t_2} dt_1 V_{fe}(t_2) V_{eg}(t_1) \chi_0(\mathbf{R}) (\mathcal{E}_s(t_2) \mathcal{E}_s(t_1) + \mathcal{E}_i(t_2) \mathcal{E}_s(t_1) + \mathcal{E}_s(t_2) \mathcal{E}_i(t_1) + \mathcal{E}_i(t_2) \mathcal{E}_i(t_1)) \quad (27)$$

where the additional terms are associated with $\mathcal{E}_i(t_2) \mathcal{E}_i(t_1)$ and $\mathcal{E}_s(t_2) \mathcal{E}_s(t_1)$. These have the same order as the desired ones absorbing signal and idler photons together, and thus cannot be eliminated by weakening the field.

2. *Selecting pathways by phase cycling*

To remove the undesired transition pathways, we can employ a phase cycling protocol [42, 43]. Phase cycling selectively extracts pathways by applying phases to the pulses,

$$\mathcal{E}_j(t) \rightarrow e^{i\theta_j} \mathcal{E}_j(t) \quad (28)$$

for $j = s, i$. It exploits the fact that different pathways respond differently to the phase change.

	θ_s	θ_i	ss	ii	si	is
I	0	$\frac{\pi}{2}$	1	-1	i	i
II	$\frac{\pi}{2}$	0	-1	1	i	i

TABLE I. Phase cycling protocol to remove additional pathways. The final signal $S = \frac{1}{2i}(S_I + S_{II})$. The four pathways are labeled by the signal (s) and idler (i) photons interacting with the molecule in the given order.

A phase cycling protocol that eliminates the two-photon transition pathways ss and ii is shown in Table I.

This protocol with Schmidt modes can be very efficient if the entangled light can be described by a limited number of Schmidt modes [44].

IV. CONCLUSIONS

We have presented a computational protocol for the entangled two-photon absorption signal in molecules which takes the nuclear quantum dynamics into account. It involves summing over all transition pathways determined by two light-matter interaction times. Using a displaced harmonic oscillator model, we have demonstrated how entangled light can be used to manipulate the two-photon-excitation process. Both electronic populations and nuclear wave packets strongly depend on the entanglement time. This protocol applies to any joint spectral amplitude of the entangled light, and thus can be applied for various sources of quantum light from e.g. cascaded emission as well. We have also outlined an alternative protocol based on the Schmidt decomposition of the

entangled light, which can be very efficient if the entangled light can be described by a limited number of Schmidt modes (weak entanglement). Our protocols allows the simulation of quantum light spectroscopy of complex molecular systems fully accounting for the coupled electronic-nuclear-photonic motion. Advances in pulse shaping techniques may allow a complete control of the JSA by varying the parameters other than entanglement time [35].

ACKNOWLEDGMENTS

We thank Dr. Feng Chen for inspiring discussions. B.G. and S.M. are supported by the National Science Foundation Grant CHE-1953045 and by the U.S. Department of Energy, Office of Science, Office of Basic Energy Sciences under Award DE-SC0020168. D.K. gratefully acknowledges support from the Alexander von Humboldt foundation through the Feodor Lynen program.

-
- [1] S. Mukamel, M. Freyberger, W. Schleich, M. Bellini, A. Zavatta, G. Leuchs, C. Silberhorn, R. W. Boyd, L. L. Sánchez-Soto, A. Stefanov, M. Barbieri, A. Paterova, L. Krivitsky, S. Shwartz, K. Tamasaku, K. Dorfman, F. Schlawin, V. Sandoghdar, M. Raymer, A. Marcus, O. Varnavski, T. Goodson, Z.-Y. Zhou, B.-S. Shi, S. Asban, M. Scully, G. Agarwal, T. Peng, A. V. Sokolov, Z.-D. Zhang, M. S. Zubairy, I. A. Vartanyants, E. del Valle, and F. Laussy, Roadmap on quantum light spectroscopy, *J. Phys. B: At. Mol. Opt. Phys.* **53**, 072002 (2020).
 - [2] K. E. Dorfman, F. Schlawin, and S. Mukamel, Nonlinear optical signals and spectroscopy with quantum light, *Rev. Mod. Phys.* **88**, 045008 (2016).
 - [3] F. Li, T. Li, M. O. Scully, and G. S. Agarwal, Quantum Advantage with Seeded Squeezed Light for Absorption Measurement, *Phys. Rev. Applied* **15**, 044030 (2021).
 - [4] O. Roslyak and S. Mukamel, A unified description of sum frequency generation, parametric down conversion and two-photon fluorescence, *Mol Phys* **107**, 265 (2009).
 - [5] F. Chen and S. Mukamel, Vibrational Hyper-Raman Molecular Spectroscopy with Entangled Photons, *ACS Photonics* (2021).
 - [6] C. K. Hong, Z. Y. Ou, and L. Mandel, Measurement of subpicosecond time intervals between two photons by interference, *Phys. Rev. Lett.* **59**, 2044 (1987).

- [7] A. Eshun, B. Gu, O. Varnavski, S. Asban, K. E. Dorfman, S. Mukamel, and T. Goodson, Investigations of Molecular Optical Properties Using Quantum Light and Hong–Ou–Mandel Interferometry, *J. Am. Chem. Soc.* **143**, 9070 (2021).
- [8] D. A. Kalashnikov, E. V. Melik-Gaykazyan, A. A. Kalachev, Y. F. Yu, A. I. Kuznetsov, and L. A. Krivitsky, Quantum interference in the presence of a resonant medium, *Sci. Rep.* **7**, 11444 (2017).
- [9] K. E. Dorfman, S. Asban, B. Gu, and S. Mukamel, Hong-Ou-Mandel interferometry and spectroscopy using entangled photons, *Commun. Phys.* **4**, 1 (2021).
- [10] T. Landes, T. Landes, M. G. Raymer, M. G. Raymer, M. Allgaier, M. Allgaier, S. Merkouche, S. Merkouche, B. J. Smith, B. J. Smith, A. H. Marcus, and A. H. Marcus, Quantifying the enhancement of two-photon absorption due to spectral-temporal entanglement, *Opt. Express, OE* **29**, 20022 (2021).
- [11] M. G. Raymer, A. H. Marcus, J. R. Widom, and D. L. P. Vitullo, Entangled Photon-Pair Two-Dimensional Fluorescence Spectroscopy (EPP-2DFS), *J. Phys. Chem. B* **117**, 15559 (2013).
- [12] H. Oka, Entangled two-photon absorption spectroscopy for optically forbidden transition detection, *J. Chem. Phys.* **152**, 044106 (2020).
- [13] F. Terenziani, C. Katan, E. Badaeva, S. Tretiak, and M. Blanchard-Desce, Enhanced Two-Photon Absorption of Organic Chromophores: Theoretical and Experimental Assessments, *Adv. Mater.* **20**, 4641 (2008).
- [14] B. R. Mollow, Two-Photon Absorption and Field Correlation Functions, *Phys. Rev.* **175**, 1555 (1968).
- [15] F. Schlawin, K. E. Dorfman, and S. Mukamel, Entangled Two-Photon Absorption Spectroscopy, *Acc. Chem. Res.* **51**, 2207 (2018).
- [16] T. Li, F. Li, C. Altuzarra, A. Classen, and G. S. Agarwal, Squeezed light induced two-photon absorption fluorescence of fluorescein biomarkers, *Appl. Phys. Lett.* **116**, 254001 (2020).
- [17] A. Eshun, Z. Cai, M. Awies, L. Yu, and T. Goodson, Investigations of Thienoacene Molecules for Classical and Entangled Two-Photon Absorption, *J. Phys. Chem. A* **122**, 8167 (2018).
- [18] K. M. Parzuchowski, A. Mikhaylov, M. D. Mazurek, R. N. Wilson, D. J. Lum, T. Gerrits, C. H. Camp Jr., M. J. Stevens, and R. Jimenez, Setting bounds on two-photon absorption cross-sections in common fluorophores with entangled photon pair excitation, (2020).
- [19] H. Oka, Highly-efficient entangled two-photon absorption with the assistance of plasmon nanoantenna, *J. Phys. B: At. Mol. Opt. Phys.* **48**, 115503 (2015).
- [20] B. Gu and S. Mukamel, Manipulating Two-Photon-Absorption of Cavity Polaritons by Entangled Light, *J. Phys. Chem. Lett.* **11**, 8177 (2020).
- [21] T. Kang, Y.-M. Bahk, and D.-S. Kim, Terahertz quantum plasmonics at nanoscales and angstrom scales, *Nanophotonics* **9**, 435 (2020).
- [22] J. Gea-Banacloche, Two-photon absorption of nonclassical light, *Phys. Rev. Lett.* **62**, 1603 (1989).
- [23] A. R. Guzman, M. R. Harpham, Ö. Süzer, M. M. Haley, and T. G. Goodson, Spatial Control of Entangled Two-Photon Absorption with Organic Chromophores, *J. Am. Chem. Soc.* **132**, 7840 (2010).

- [24] O. Varnavski and T. Goodson, Two-Photon Fluorescence Microscopy at Extremely Low Excitation Intensity: The Power of Quantum Correlations, *J. Am. Chem. Soc.* **142**, 12966 (2020).
- [25] S. Szoke, M. He, B. P. Hickam, and S. K. Cushing, Designing High-Power, Octave Spanning Entangled Photon Sources for Quantum Spectroscopy, , 10 (2021).
- [26] H.-B. Fei, B. M. Jost, S. Popescu, B. E. A. Saleh, and M. C. Teich, Entanglement-Induced Two-Photon Transparency, *Phys. Rev. Lett.* **78**, 1679 (1997).
- [27] D.-I. Lee and T. Goodson, Entangled Photon Absorption in an Organic Porphyrin Dendrimer, *J. Phys. Chem. B* **110**, 25582 (2006).
- [28] D. Tabakaev, M. Montagnese, G. Haack, L. Bonacina, J.-P. Wolf, H. Zbinden, and R. T. Thew, Energy-time-entangled two-photon molecular absorption, *Phys. Rev. A* **103**, 033701 (2021).
- [29] J. Javanainen and P. L. Gould, Linear intensity dependence of a two-photon transition rate, *Phys. Rev. A* **41**, 5088 (1990).
- [30] C. Couteau, Spontaneous parametric down-conversion, *Contemporary Physics* **59**, 291 (2018), [arXiv:1809.00127](https://arxiv.org/abs/1809.00127).
- [31] M. H. Rubin, D. N. Klyshko, Y. H. Shih, and A. V. Sergienko, Theory of two-photon entanglement in type-II optical parametric down-conversion, *Phys. Rev. A* **50**, 5122 (1994).
- [32] M. H. Rubin, Transverse correlation in optical spontaneous parametric down-conversion, *Phys. Rev. A* **54**, 5349 (1996).
- [33] T. E. Keller and M. H. Rubin, Theory of two-photon entanglement for spontaneous parametric down-conversion driven by a narrow pump pulse, *Phys. Rev. A* **56**, 1534 (1997).
- [34] A. Muthukrishnan, G. S. Agarwal, and M. O. Scully, Inducing Disallowed Two-Atom Transitions with Temporally Entangled Photons, *Phys. Rev. Lett.* **93**, 093002 (2004).
- [35] F. Schlawin, Entangled photon spectroscopy, *J. Phys. B: At. Mol. Opt. Phys.* **50**, 203001 (2017).
- [36] S. Mukamel, *Principles of Nonlinear Optical Spectroscopy* (Oxford University Press, 1995).
- [37] R. J. Glauber, The Quantum Theory of Optical Coherence, *Phys. Rev.* **130**, 2529 (1963).
- [38] S. P. Walborn, C. H. Monken, S. Pádua, and P. H. Souto Ribeiro, Spatial correlations in parametric down-conversion, *Physics Reports* **495**, 87 (2010).
- [39] R. Kosloff, Time-dependent quantum-mechanical methods for molecular dynamics, *J. Chem. Phys.* **92**, 2087 (1988).
- [40] C. K. Law and J. H. Eberly, Analysis and Interpretation of High Transverse Entanglement in Optical Parametric Down Conversion, *Phys. Rev. Lett.* **92**, 127903 (2004).
- [41] M. G. Raymer and I. A. Walmsley, Temporal Modes in Quantum Optics: Then and Now, (2019).
- [42] H.-S. Tan, Theory and phase-cycling scheme selection principles of collinear phase coherent multi-dimensional optical spectroscopy, *The Journal of Chemical Physics* **129**, 124501 (2008).
- [43] D. Cho, J. R. Rouxel, M. Kowalewski, P. Saurabh, J. Y. Lee, and S. Mukamel, Phase Cycling RT-TDDFT Simulation Protocol for Nonlinear XUV and X-ray Molecular Spectroscopy, *J. Phys. Chem.*

Lett. **9**, 1072 (2018).

- [44] J. H. Eberly, Schmidt Analysis of Pure-State Entanglement, Laser Phys. **16**, 921 (2006), [arXiv:quant-ph/0508019](#).